Hindawi
Advances in Tribology
Volume 2023, Article ID 1520135, 9 pages
https://doi.org/10.1155/2023/1520135

Research Article

Tribological and Mechanical Properties of Gradient Coating on Al_2O_3-Based Coating Produced by Detonation Spraying Methods

B. K. Rakhadilov,[1] D. N. Kakimzhanov,[1] D. B. Buitkenov,[2] R. S. Kozhanova,[3] L. G. Zhurerova,[2] and Zh. B. Sagdoldina[2]

[1]PlasmaScience LLP, Ust-Kamenogorsk, Kazakhstan
[2]Sarsen Amanzholov East Kazakhstan University, Ust-Kamenogorsk, Kazakhstan
[3]Shakarim State University of Semey, Semey, Kazakhstan

Correspondence should be addressed to D. N. Kakimzhanov; dauir_97@mail.ru

Received 12 August 2023; Revised 19 October 2023; Accepted 9 November 2023; Published 28 November 2023

Academic Editor: Patrick De Baets

This work is aimed at obtaining gradient coating of aluminum oxide (Al_2O_3) by detonation spraying. The influence of technological parameters of spraying on the formation of structure, phase composition. mechanical, and tribological characteristics of Al_2O_3 coatings have been investigated. It was determined that coatings obtained from the same raw powder materials under different technological conditions show different structural and phase characteristics. X-ray diffraction analysis showed that when the barrel is filled with gas mixture by 56%, the coating with the main phase α-Al_2O_3 is formed, and when the barrel is filled with gas mixture by 63%, the coating with the main phase γ-Al_2O_3, which is relatively more ductile than α-Al_2O_3, is formed. It is determined that the α-Al_2O_3 formed mainly on the surface provides good wear resistance. The bottom layer composed of γ-Al_2O_3 phase, which is relatively more ductile than α-Al_2O_3, provides good adhesion of the coating to the substrate. Tribological study showed that the coating obtained at 56% of filling shows good wear resistance compared to other samples. At 63% of filling the results of scratch test showed good adhesive strength. By varying the technological mode of detonation sputtering (56%, 53%, and 63%), Al_2O_3 coating with gradient structure was obtained, in which γ-Al_2O_3 smoothly transitions to α-Al_2O_3 from the substrate to the surface. The hardness of the coatings was found to increase smoothly from substrate to surface (12.4–14.2 GPa).

1. Introduction

The condition of material surfaces is of crucial importance in modern mechanical engineering as it affects the functionality of machine and tool parts. The surface layers of these parts are particularly vulnerable to wear during operation. To improve physical and mechanical properties of metals and alloys, protective coatings with high strength, wear resistance and resistance to aggressive media, low thermal, and electrical conductivity are used. This significantly increases the service life and reliability of structural parts. For the manufacture of protective coatings that meet these requirements, oxide-aluminum ceramics are usually used. Aluminum oxide coatings are particularly useful for improving the performance of metals in high-temperature and aggressive environments due to their high chemical and thermal stability [1].

The physical and mechanical characteristics of aluminum oxide coatings can be improved by increasing the proportion of α-Al_2O_3 in the coating composition. Usually, bulk or surface heat treatment is used to obtain α-Al_2O_3. However, this increases the labor intensity of the coating process and is not economically feasible.

The phase composition of aluminum oxide coatings is influenced by many factors, such as deposition method, process parameters, substrate temperature, particle size, and many others. Standard methods of obtaining such coatings include microarc oxidation [4, 5], anodic oxidation [6, 7], sol–gel [8, 9], plasma [10–12], and gas-flame deposition [2, 13, 14], as well as detonation sputtering [15, 16]. A relatively new direction in this field is the use of detonation technology, which refers to gas-thermal methods of coating modification. This method makes it possible to create high-quality coatings with lower energy costs and less components

Table 1: Chemical composition of 12X18H10T steel (AISI 321).

C	Si	Mn	P	S	Cr	Mo	Ni	V	Ti	Cu	W	Fe
<0.12	<0.8	<2.0	<0.035	<0.02	17.0–19.0	<0.5	9.0–11.0	<0.2	<0.8	<0.4	<0.2	The rest

in the gas mixture, compared to other methods of gas-thermal deposition, and at the same time provides the possibility of producing coatings up to 500 μm thick at the industrial level [16]. Plasma and detonation spraying methods are of particular interest. For example, when α-Al_2O_3 is used as a starting powder to create aluminum oxide coatings using gas-flame spraying, the resulting coating is mainly composed of γ-Al_2O_3. Meanwhile, plasma and detonation sputtering produce biphasic coatings that include both α-Al_2O_3 and γ-Al_2O_3 [14, 16]. It is important to note that the coatings obtained by these methods often contain the main phase γ-Al_2O_3, which is characterized by a less dense structure and lower hardness, wear resistance, and corrosion resistance compared to α-Al_2O_3 [19–20].

Recent studies [21, 22] also indicate that it is possible to obtain coatings with the main α-Al_2O_3 phase by plasma spraying using γ-Al_2O_3 as a starting powder. These studies show that the variation of process parameters, such as firing frequency and barrel fill volume, affects the ratio of α-Al_2O_3 and γ-Al_2O_3 phases in the resulting coatings. Consequently, the structural and phase characteristics of aluminum oxide coatings are significantly affected by the technological parameters of detonation spraying. Our previous studies [23–25] also confirmed that changes in parameters such as the explosion frequency and the volume filled with the gas mixture in the barrel lead to changes in the content of α-Al_2O_3 and γ-Al_2O_3 phases in the coatings. In our studies [23–25], we used α-Al_2O_3 as a starting powder and investigated the effects of maximum parameters on a CCDS2000 detonation machine. We found that as the blast frequency decreases, the α-Al_2O_3 content of the coatings increases. However, the main phase remains γ-Al_2O_3. Despite the positive results obtained in the current research on detonation coatings of aluminum oxide, it is important to note that there is still a need to increase the α-Al_2O_3 content in such coatings, since this phase has excellent physical and mechanical properties. Based on the available literature, data on detonation coatings having α-Al_2O_3 as the main phase are still lacking. Our previously published work [24] reported results on the production of aluminum oxide coatings having α-Al_2O_3 as the main phase by optimizing detonation sputtering process regimes. In this work, we studied the tribological and mechanical properties of a gradient coating based on Al_2O_3 obtained by detonation sputtering.

2. Materials and Methods

Corundum (α-Al_2O_3) powder [26–27] with a dispersity of 20–45 μm of spherical shape (LLC STC "INOX") was used as the sputtering material. Stainless steel 12X18H10T (AISI 321) was used as the substrate material. The chemical composition of 12Cr18Ni10Ti steel is shown in Table 1.

The coatings were applied to the samples by detonation spraying on a CCDS2000 (computer-controlled detonation spraying) machine [28]. Figure 1 shows the general view and schematic diagram of the detonation complex CCDS2000. The coating is applied by a detonation gun, the barrel of which is filled with an explosive gas mixture, a dosed portion of powder is thrown into the barrel, and detonation is excited by an electric spark. The detonation product heats the powder particles to melting and throws them at high velocity at the part mounted in front of the gun barrel. Upon impact, microwelding occurs and the powder is firmly (at the molecular level) bonded to the surface of the part. After each shot, the barrel is purged with nitrogen, to clean the residue of detonation products. The required thickness is built up by a series of consecutive shots, during which the object can be moved with the help of a manipulator [29].

Gradient coatings based on Al_2O_3 were applied to samples of AISI 321 steel by our developed method [24]. The developed method includes abrasive blasting and coating using α-Al_2O_3 powder by impacting the treated surface with a stream of heated powder particles formed in the barrel of the detonation spraying machine. At the same time, the surface blasting and coating are carried out sequentially at different regimes of detonation spraying using the same α-Al_2O_3 powder. The regime of surface abrasive treatment is selected so that the abrasive particles reach the surface to be sprayed in solid state and atomize the surface. Coating is carried out by stepwise changing the regime of detonation spraying to obtain a gradient structure in which γ-Al_2O_3 smoothly transitions to α-Al_2O_3 from the substrate to the surface, and the spraying process includes the following continuous steps: first stage—the volume of filling the barrel with acetylene and oxygen gas mixture is 63%, second stage—the volume of filling the barrel with acetylene and oxygen gas mixture is 53%, and third stage—the volume of filling the barrel with acetylene, oxygen, and propane gas mixture is 56%.

Table 2 shows the spraying regimes. For samples nos. 1–3 the aluminum oxide coating was obtained by detonation spraying at different filling volumes of 63%, 56%, and 53%, respectively. When spraying sample no. 4, the process parameters are gradually changed and the spraying regime includes three continuous stages 63%, 53%, and 56% to obtain a gradient coating.

X-ray phase studies of the samples were performed by X-ray diffraction analysis on a X'PertPRO diffractometer (Philips Corporation, Netherlands). The diffractograms were taken using CuKα-radiation ($\lambda = 2.2897$ A°) at a voltage of 40 kV and a current of 30 mA. The diffractograms were decoded using the HighScore program. Mechanical properties of the obtained coatings (Young's modulus, hardness) were investigated using a NanoScan-4D Compact nanohardness tester (FSBI "TISNUM," Russia). Nanoindentation of coatings was carried out according to the method of Oliver and Farr using Berkovich indenter at a load of 100 mN (ASTM

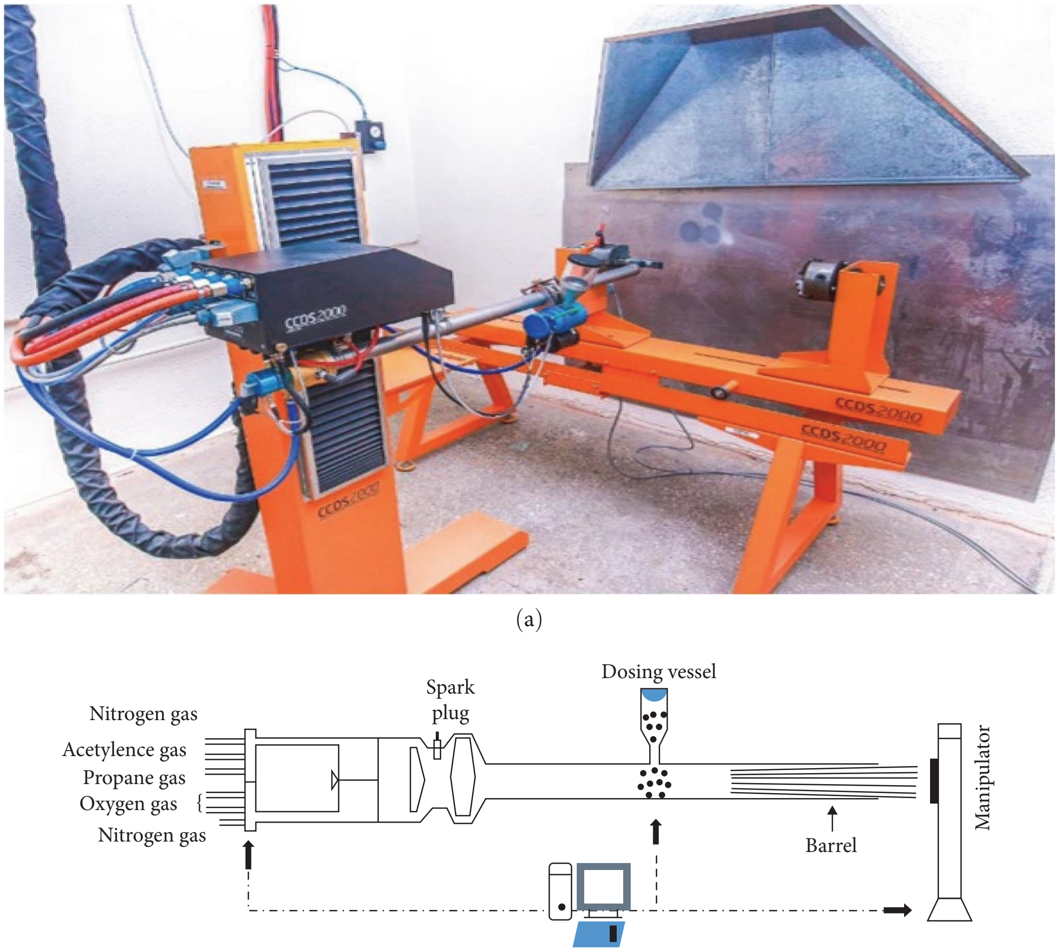

(a)

(b)

Figure 1: Computerized detonation complex CCDS2000: (a) general view and (b) schematic diagram of the setup.

Table 2: Technological regimes for spraying aluminum oxide coatings.

Sample no.	Fuel/oxidizer ratios	Barrel fill volume (%)	Spray distance (mm)	Number of shots
1	1.856	63	250	15
2	1.856	56	250	15
3	1.026	53	250	15
4	1.856–1.026	63–53–56	250	15

E2546-07). The surface roughness of the coatings Ra was evaluated using a profilometer model 130 (JSC "Plant PROTON," Moscow, Russia). The Ra value, which represents the arithmetic mean deviation of the profile, was chosen as the main parameter for evaluating the coating surface roughness. Three measurements were made to obtain the surface roughness value for each sample.

Microhardness of the cross-section of the samples was measured in accordance with GOST 9450-76 (ASTM E384-11) on a microtweedometer Metolab 502 (Metolab, Russia), at indenter load $P = 1$ N and dwell time 10 s.

Tribological tests on sliding friction were carried out on tribometer TRB^3 (Anton Paar Srl, Peseux, Switzerland) using the standard method "ball-on-disk" (international standards ASTM G 133-95 and ASTM G99). A 3.0-mm diameter ball made of SiC-coated steel was used as a counterbody at a load of 5 N and linear velocity of 15 cm/s, wear curvature radius of 5 mm, and friction path of 50 m. According to the obtained profilometer values, profilograms were plotted, and using a special program, values for calculating the wear volumes of the obtained coatings were obtained.

To investigate the adhesion characteristics of coatings by "scratching" method a scratch tester CSEM micro-scratch tester (Neuchatel, Switzerland) was used. Scratch tests were carried out at a maximum load of 30 N, the change in the rate of normal load on the sample was 29.99 N/min, the indenter displacement speed was 9.63 mm/min, the scratch length was 10 mm, and the tip radius of curvature was 100 μm.

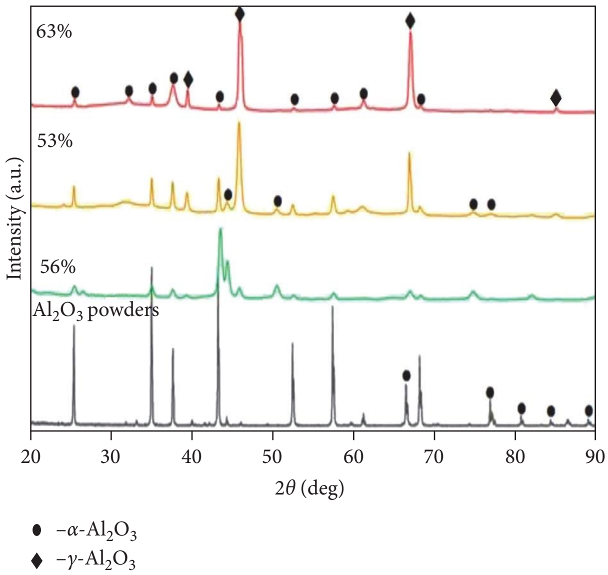

Figure 2: Diffractograms of Al_2O_3-based coatings obtained at different fillings of the detonation spraying barrel.

Surface morphology was studied by scanning electron microscopy on a MIRA scanning electron microscope (SEM) MIRA SEM (Tescan, Czech Republic).

3. Results and Discussion

Al_2O_3 coatings were obtained by varying the volume of barrel filling. At standard regimes of detonation spraying using initial powder from α-Al_2O_3, the obtained coatings have the main phase of γ-Al_2O_3. In order to obtain coatings with α-Al_2O_3 basic phase, we conducted a series of experiments in different detonation spraying regimes. Figure 2 shows the diffractograms of the obtained coatings. The results of X-ray diffraction analysis of the coatings showed that 63% of the barrel filling yielded a coating with γ-Al_2O_3 main phase, and 56% of the barrel filling yielded a coating with α-Al_2O_3 main phase and 53% of the barrel filling yielded a coating with α-Al_2O_3 and γ-Al_2O_3 main phase (ICDD card number 96-500-0093). This is explained by the fact that nonequilibrium recrystallization of α-Al_2O_3 phase to γ-Al_2O_3 phase occurs under shock wave conditions and rapid cooling during coating formation. To calculate the content of α-Al_2O_3 phase in the coatings, a semicrystallization analysis was performed [27].

$$C_\alpha = \frac{I(104) + I(113) + I(116)}{I(104) + I(113) + I(116) + I(311) + I(400) + I(440)}, \quad (1)$$

where C_α represents the content of α-Al_2O_3 phase and I represents peak area.

The results of semicrystal analysis show that the content of α-Al_2O_3 phase in the coating obtained at 56% barrel filling (α-Al_2O_3—78.62%) is much higher than at 53% (α-Al_2O_3—60.96%) and 63% (α-Al_2O_3—23.4%).

Figure 3 shows the microstructure of the coatings and the results of measuring the surface roughness of the Al_2O_3-based coating material.

Metallographic analysis showed that the coatings have a heterogeneous structure with the presence of small pores. The pore size and number of pores in the coating obtained at 56% barrel fill are larger than those obtained at 53% and 63%. The roughness parameter of the coating obtained at 63% filling of the barrel has a value of $R_a = 1.72 \pm 0.0286\,\mu m$ (Figure 3(a)), and the coating at 56% has a value of $R_a = 3.85 \pm 0.0273\,\mu m$ (Figure 3(b)) and the coating at 53% has a value of $Ra = 1.72 \pm 0.0276\,\mu m$ (Figure 3(c)). The high roughness and porosity of the coating obtained at 56% barrel filling are due to the difference in the impact of the shock wave and the resulting compaction of the coating.

One of the main factors determining the quality of the coating is adhesion. Figure 4 shows the adhesion test results for the scratch test. The moment of adhesion or cohesive failure of the coating was recorded by changing two parameters: acoustic emission (AE) and friction force.

It should be noted that not all the recorded coating failure events describe the actual adhesion of the coating to the substrate. Different registration parameters during the tests allowed to record different stages of coating failure. So, Lc1 means the moment of the first crack appearance, Lc2 peeling of coating sections, and Lc3-plastic abrasion of the coating against the substrate [17]. The type of change in the amplitude of AE can be used to judge the intensity of crack formation and their development in the sample during scratching. In the coating obtained by filling the barrel by 56%, the first crack was formed at a load Lc1 = 6 N (Figure 4(a)). Then the process continued in a certain cycle. The corresponding AE peak accompanied the formation of each crack (Figure 4(a)). Partial abrasion of the coating against the substrate was judged by a sharp change in the intensity of friction force growth. This occurred at the load Lc3 = 29 N. In the coating obtained by filling the barrel by 53%, the first crack was formed at the load Lc1 = 10 N (Figure 4(b)) In the coating obtained by filling the barrel by 63%, the first crack was formed at the load Lc1 = 15 N (Figure 4(c)). According to the results of adhesion tests, it can be stated that the cohesive failure of the sample coating occurred at 15 N, and its adhesive failure occurred at 29 N. The coatings obtained at 63% barrel filling have good adhesion strength than the coatings obtained at 53% and 56% barrel filling. This is due to the fact that the coating obtained at 63% barrel filling has γ-Al_2O_3 as the main phase, which is relatively more ductile than the α-Al_2O_3 phase and this provides good adhesion of the coating to the substrate.

The Vickers method was used to determine the hardness of Al_2O_3 detonation coatings obtained at different borehole fillings. The results of hardness measurement are shown in Figure 5. The hardness of coatings at 56% borehole filling has the highest hardness (14.1 GPa). This is due to the increased proportion of α-Al_2O_3 phase in the coating obtained at 56% barrel filling, which has high wear resistance. At 53% and 63% of barrel filling hardness decreases 13.6 and 12.4 GPa, respectively, this is due to a decrease in the proportion of α-Al_2O_3 phase in the coating.

One of the main properties responsible for the durability of products is tribological parameters, which in this work were evaluated by the value of the wear volume of coatings during

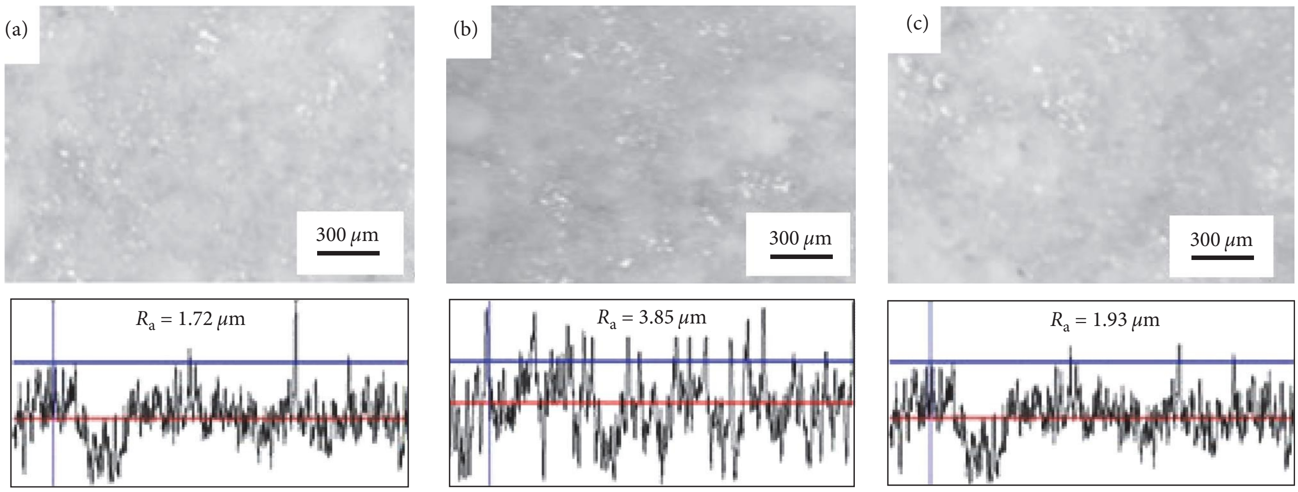

FIGURE 3: Micrographs of topography and surface roughness of coatings 63% (a), 53% (b), and 56% (c).

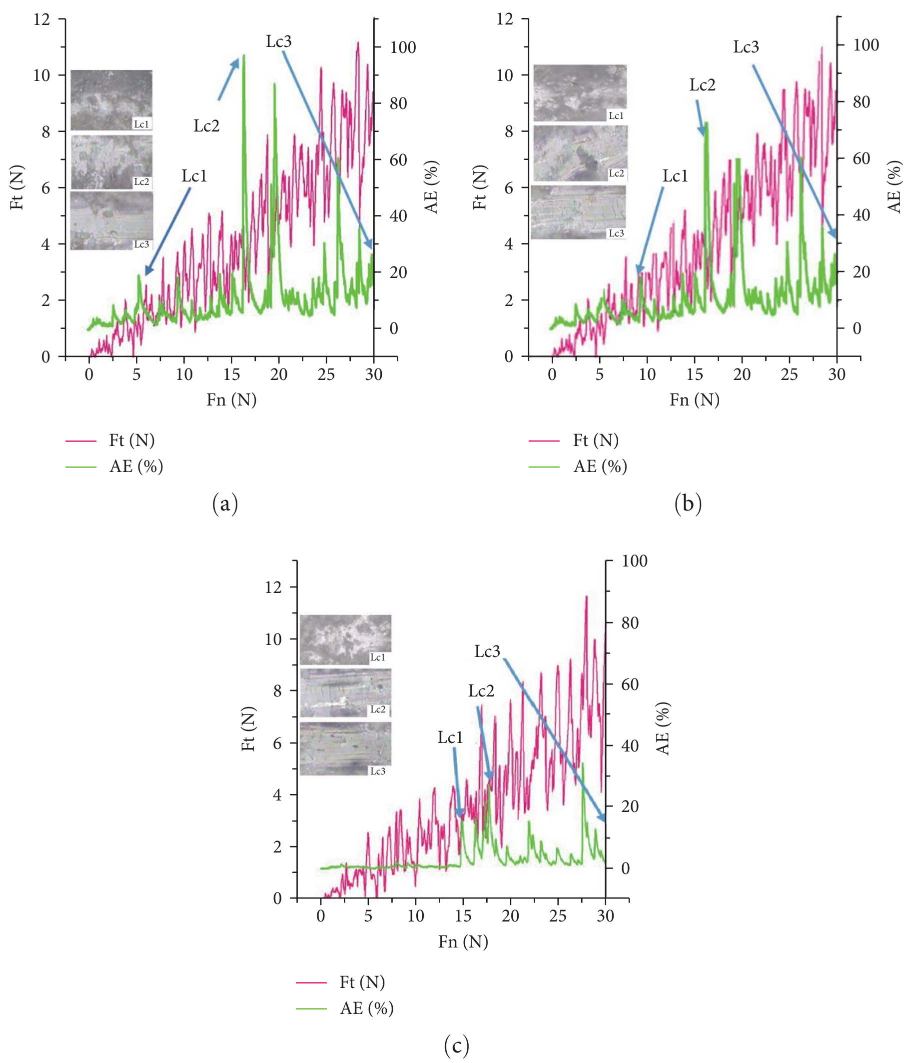

FIGURE 4: Coverage scratch test results 56% (a), 53% (b), and 63% (c).

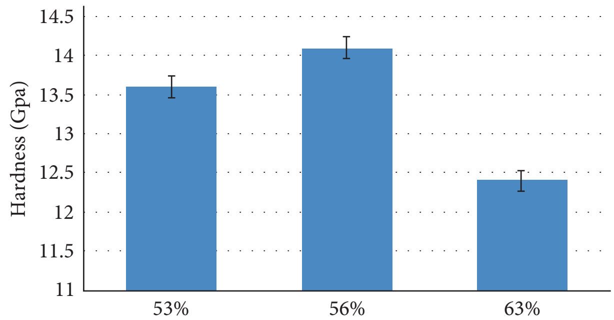

FIGURE 5: Hardness results of coatings Al_2O_3.

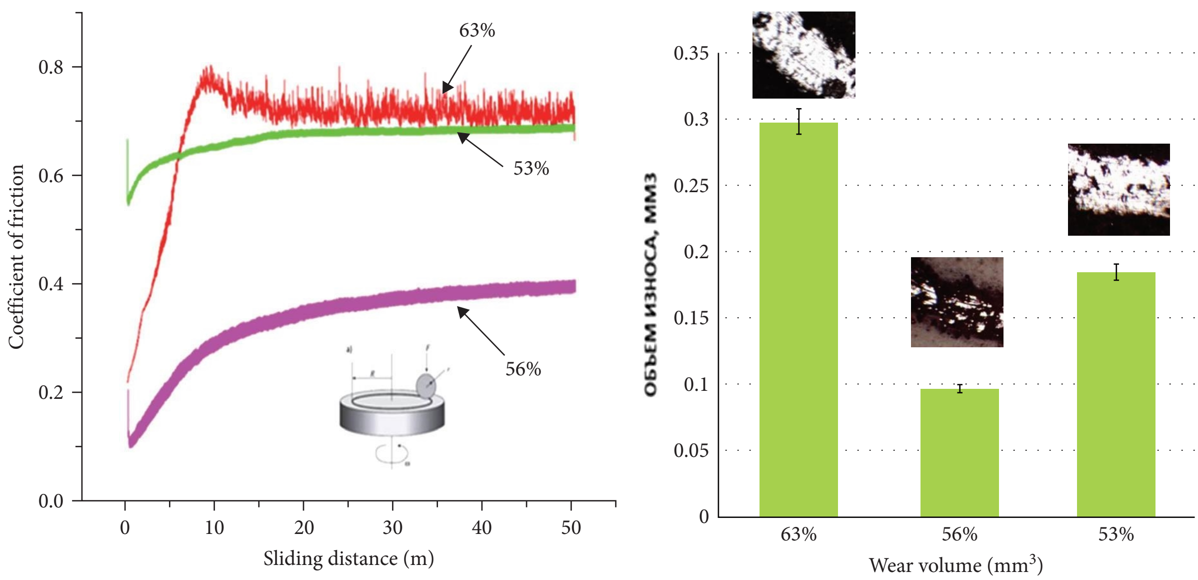

(a) (b)

FIGURE 6: Friction coefficient (a) and wear volume (b) of coatings obtained at different detonation barrel fillings.

the "ball-on-disk" test. Figure 6 shows the data on the wear volume (Figure 6(b)) and friction coefficient (Figure 6(a)) of the coatings at different detonation barrel fills. Also the figure shows the wear morphology of the obtained coatings [31, 32]. The test results show that the sample obtained at 56% barrel filling has a low value of wear volume compared to the samples obtained at 63% and 53% barrel fillings. Figure 6(a) shows that the coefficient of friction of the sample obtained at 63% barrel filling is 0.68, and at 53% barrel filling is 0.61, and the coefficient of friction of the sample obtained at 56% barrel filling is 0.32. Thus, it can be stated that under the tested conditions, the wear resistance of the sample obtained at 56% barrel filling is three times higher than that obtained at 63% and 53%. This is primarily due to the increased proportion of α-Al_2O_3 phase in the coating obtained at 56% barrel filling, which has a high resistance to wear.

Based on the study of the influence of the spraying regime on the structure and properties of Al_2O_3 coatings, we developed a method for obtaining gradient coatings. This method uses a CCDS2000 detonation complex and Al_2O_3-based powder; the technological parameters are varied during the spraying process. We gradually varied the barrel filling volume, i.e., the first layer was sprayed at 63% barrel filling, followed by the second layer at 53% and the third layer on the surface at 56% barrel filling, and then studied the structure and properties of the resulting Al_2O_3-based gradient coating. The choice of spraying regime is based on the experimental results presented above and is aimed at obtaining coatings in which the content of the α-Al_2O_3 phase fraction increases uniformly from the substrate to the coating surface. The volume fraction of α-Al_2O_3 phase formed on the surface provides good wear resistance. The bottom layer consists of γ-Al_2O_3 phase, which is relatively more ductile than α-Al_2O_3 phase and provides good adhesion of the coating to the substrate.

Figure 7 shows a plot of the distribution of instrumental nanoindentation and elastic modulus over the thickness of the Al_2O_3-based gradient coating. As can be seen, the

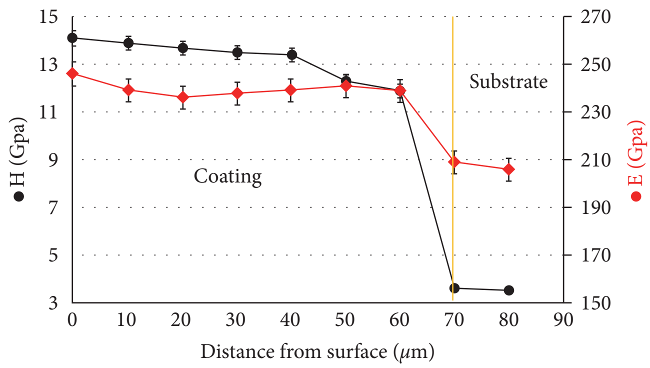

FIGURE 7: Graph of hardness and elastic modulus distribution by depth of gradient coating on the basis of Al_2O_3.

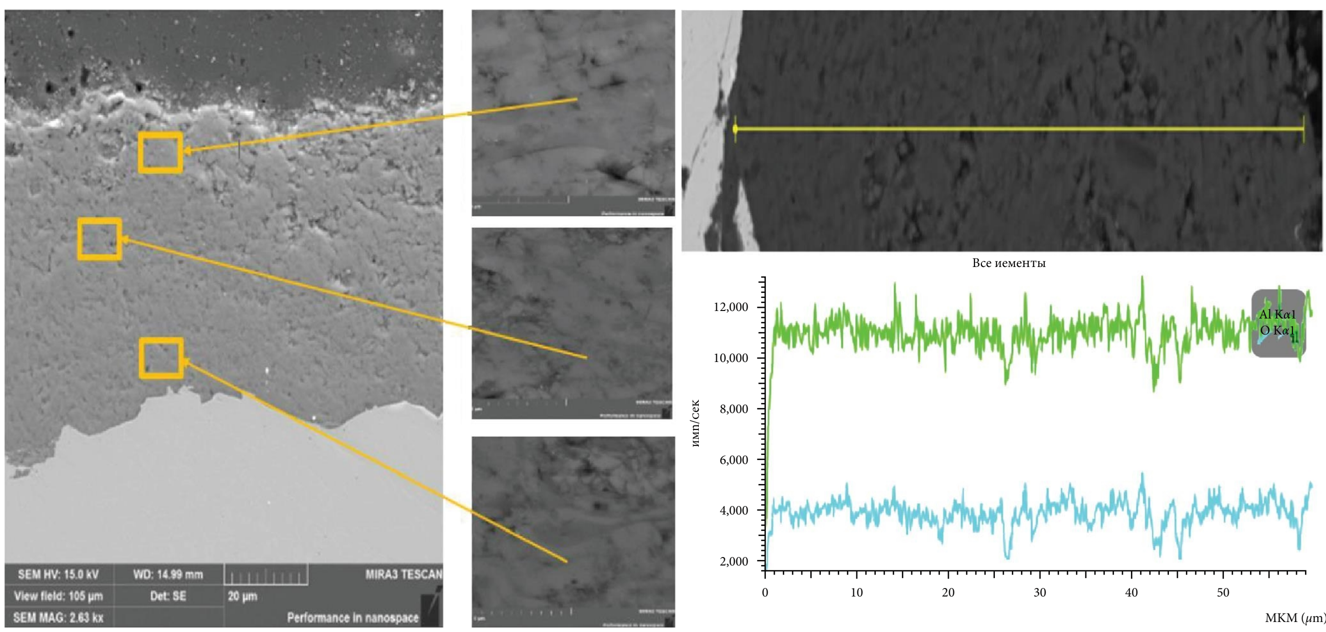

FIGURE 8: SEM images of cross-section and feature distribution as a function of depth of the Al_2O_3-based gradient coating.

hardness values increase smoothly from substrate to surface. The maximum hardness value is 14.2 GPa. The values of elastic modulus are from 200 to 250 GPa. The hardness of coatings obtained by the proposed method is distributed from the surface to the substrate in the following way: on the surface of the coating hardness has a maximum value, then smoothly decreases down to the substrate. In this case, near the substrate hardness is 3.5–4 GPa, which is comparable to the hardness of most steels. This prevents cracking and delamination of coatings. Thus, high hardness of the coating surface and smooth decrease of hardness along the coating depth provides high-performance properties of the parts, on the surface of which this coating is applied. In addition, due to the formation of α-Al_2O_3 on the surface layer, high mechanical and tribological characteristics of coatings are provided. The formation of γ-Al_2O_3 on the substrate–coating interface provides high adhesion strength of the coating.

Figure 8 shows SEM images of the cross-section of the Al_2O_3-based gradient coating. The thickness of the coating is ~60–70 μm. As can be seen from the obtained gradient coating has an integral (not layered) structure characterized by a smooth transition (gradient) of phase composition between the main zones formed under different spraying regimes. Practically no boundary between the layers obtained after the first, second, and third stages of detonation spraying of aluminum oxide by the proposed method is observed.

4. Conclusion

Based on the conducted study of the influence of the spraying regime on the structure and properties of Al_2O_3 coatings, we can state that the phase composition and properties of detonation coatings strongly depend on the technological parameters of spraying. When spraying Al_2O_3-based powder, the chemical and phase composition of the resulting coatings strongly depends on the degree of filling of the barrel with gas mixture. It has been determined that the coating having α-Al_2O_3 basic phase has high hardness, wear resistance, and erosion resistance in comparison with the coating having γ-Al_2O_3 basic phase. It is determined that the coating having γ-Al_2O_3 basic phase has high adhesion strength compared to the coating having α-Al_2O_3 basic phase. Thus, the results showed that it is possible to control the phase composition of Al_2O_3-based coatings and, consequently, the properties of the coatings by changing the composition and filling degree of the combustible mixtures. For the first time experimentally obtained a gradient coating in which the content of α-Al_2O_3 fractions increases uniformly from the substrate to the coating surface The volumetric fraction of α-Al_2O_3 formed on the surface provides good wear resistance. The bottom layer is composed of γ-Al_2O_3 phase, which is relatively more ductile than α-Al_2O_3 and provides good adhesion of the coating to the substrate.

Data Availability

The (all type) data used to support the findings of this study are included within the article.

Disclosure

The authors confirm that this work does not contain any studies with human participants performed by any of the authors.

Conflicts of Interest

The authors declare that there is no conflict of interest regarding the publication of this manuscript.

Acknowledgments

This research is funded by the Science Committee of the Ministry of Science and Higher Education of the Republic of Kazakhstan (grant no. AP09058615) and also within the framework of the International Innovative Nanotechnology Centre of the CIS countries grant no. 23-108 from 05.05.2023.

References

[1] B. Dhakar, S. Chatterjee, and K. Sabiruddin, "Measuring mechanical properties of plasma-sprayed alumina coatings by nanoindentation technique," *Materials Science and Technology*, vol. 33, no. 3, pp. 285–293, 2017.

[2] J. W. Murray, A. S. M. Ang, Z. Pala, E. C. Shaw, and T. Hussain, "Suspension high velocity oxy-fuel (SHVOF)-sprayed alumina coatings: microstructure, nanoindentation and wear," *Journal of Thermal Spray Technology*, vol. 25, no. 8, pp. 1700–1710, 2016.

[3] M. Nofz, I. Dörfel, R. Sojref, N. Wollschläger, M. Mosquera-Feijoo, and A. Kranzmann, "Microstructure, smoothening effect, and local defects of alumina sol-gel coatings on ground steel," *Journal of Sol-Gel Science and Technology*, vol. 81, no. 1, pp. 185–194, 2017.

[4] S. Yizhou, T. Haijun, L. Yuebin et al., "Fabrication and wear resistance of TiO_2/Al_2O_3 coatings by micro-arc oxidation," *Rare Metal Materials and Engineering*, vol. 46, no. 1, pp. 23–27, 2017.

[5] Y. L. Wang, M. Wang, M. Zhou, B. J. Li, G. Amoako, and Z. H. Jiang, "Microstructure characterisation of alumina coating on steel by PEO," *Surface Engineering*, vol. 29, no. 4, pp. 271–275, 2013.

[6] L. D. Rafailović, C. Gammer, C. Rentenberger, T. Trišović, C. Kleber, and H. P. Karnthaler, "Functionalizing aluminum oxide by Ag dendrite deposition at the anode during simultaneous electrochemical oxidation of Al," *Advanced Materials*, vol. 27, no. 41, pp. 6438–6443, 2015.

[7] H. Masuda, H. Yamada, M. Satoh, H. Asoh, M. Nakao, and T. Tamamura, "Highly ordered nanochannel-array architecture in anodic alumina," *Applied Physics Letters*, vol. 71, no. 19, pp. 2770–2772, 1997.

[8] I. B. Singh, O. P. Modi, and G. Ruhi, "Development of sol–gel alumina coating on 9Cr–1Mo ferritic steel and their oxidation behavior at high temperature," *Journal of Sol-Gel Science and Technology*, vol. 74, no. 3, pp. 685–691, 2015.

[9] N. Wollschläger, M. Nofz, I. Dörfel, W. Schulz, R. Sojref, and A. Kranzmann, "Exposition of sol-gel alumina-coated P92 steel to flue gas: time-resolved microstructure evolution, defect tolerance, and repairing of the coating," *Materials and Corrosion*, vol. 69, no. 4, pp. 492–502, 2018.

[10] M. Djendel, O. Allaoui, and R. Boubaaya, "Characterization of alumina-titania coatings produced by atmospheric plasma spraying on 304 SS steel," *Acta Physica Polonica A*, vol. 132, no. 3, pp. 538–540, 2017.

[11] Z. Yin, S. Tao, X. Zhou, and C. Ding, "Tribological properties of plasma sprayed Al/Al_2O_3 composite coatings," *Wear*, vol. 263, no. 7–12, pp. 1430–1437, 2007.

[12] B. K. Rakhadilov, Y. Tyurin, D. Kakimzhanov, D. Baizhan, O. Kolisnichenko, and L. Zhurerova, "Deposition of duplex Cr3C2-NiCr coatings on steel using a combined technique of gas detonation spraying and pulse-plasma treatment," *High Temperature Material Processes: An International Quarterly of High-Technology Plasma Processes*, vol. 25, no. 4, pp. 25–37, 2021.

[13] C.-J. Li, J. Zou, H.-B. Huo, J.-T. Yao, and G.-J. Yang, "Microstructure and properties of porous abradable alumina coatings flame-sprayed with semi-molten particles," *Journal of Thermal Spray Technology*, vol. 25, no. 1-2, pp. 264–272, 2016.

[14] S.-K. Jia, Y. Zou, J.-Y. Xu, J. Wang, and L. Yu, "Effect of TiO_2 content on properties of Al_2O_3 thermal barrier coatings by plasma spraying," *Transactions of Nonferrous Metals Society of China*, vol. 25, no. 1, pp. 175–183, 2015.

[15] V. Y. Ulianitsky, A. A. Shtertser, I. S. Batraev, and D. K. Rybin, "Fabrication of layered ceramic–metal composites by detonation spraying," *Ceramics International*, vol. 46, no. 17, pp. 27903–27908, 2020.

[16] V. Ulianitsky, A. Shtertser, S. Zlobin, and I. Smurov, "Computer-controlled detonation spraying: from process fundamentals toward advanced applications," *Journal of Thermal Spray Technology*, vol. 20, no. 4, pp. 791–801, 2011.

[17] O. Zywitzki and G. Hoetzsch, "Effect of plasma activation on the phase transformations of aluminum oxide," *Surface and Coatings Technology*, vol. 76-77, Part 2, pp. 754–762, 1995.

[18] H. C. Lin, P. D. Ye, and G. D. Wilk, "Leakage current and breakdown electric-field studies on ultrathin atomic-layer-deposited Al_2O_3 on GaAs," *Applied Physics Letters*, vol. 87, Article ID 182904, 2005.

[19] K. Sabiruddin, J. Joardar, and P. P. Bandyopadhyay, "Analysis of phase transformation in plasma sprayed alumina coatings using Rietveld refinement," *Surface and Coatings Technology*, vol. 204, no. 20, pp. 3248–3253, 2010.

[20] A. Vardelle, M. Vardelle, and P. Fauchais, "Influence of velocity and surface temperature of alumina particles on the

properties of plasma sprayed coatings," *Plasma Chemistry and Plasma Processing*, vol. 2, no. 3, pp. 255–291, 1982.

[21] B. Niu, L. Qiang, J. Zhang et al., "Plasma sprayed α-Al_2O_3 main phase coating using γ-Al_2O_3 powders," *Surface Engineering*, vol. 35, no. 9, pp. 801–808, 2019.

[22] L. Qiang, X. Zhang, Y. Ai et al., "In situ deposition of amorphous Al_2O_3-GAP ceramic coating with excellent microstructure stability and uniformity via atmospheric plasma spraying," *Coatings*, vol. 12, no. 2, Article ID 119, 2022.

[23] B. Rakhadilov, D. Kakimzhanov, D. Baizhan, G. Muslimanova, S. Pazylbek, and L. Zhurerova, "Comparative study of structures and properties of detonation coatings with α-Al_2O_3 and γ-Al_2O_3 main phases," *Coatings*, vol. 11, no. 12, Article ID 1566, 2021.

[24] B. K. Rakhadilov, D. R. Baizhan, and D. N. Kakimzhanov, "Method of detonation coating of aluminum oxide," *Patent of the Republic of Kazakhstan*, No. 36130, 2023.

[25] N. Kantay, B. Rakhadilov, S. Kurbanbekov, D. Yeskermessov, G. Yerbolatova, and A. Apsezhanova, "Influence of detonation-spraying parameters on the phase composition and tribological properties of Al_2O_3 coatings," *Coatings*, vol. 11, no. 7, Article ID 793, 2021.

[26] Y. Wang, L. Zhang, A. Liu, C. Wu, and W. Li, "Tribological performance of silicone oil based Al_2O_3 nano lubricant for an Mg alloy subjected to sliding at elevated temperatures," *Tribology International*, vol. 175, Article ID 107779, 2022.

[27] Y. Wang, L. Zhang, A. Liu, and C. Wu, "Tribological performance for an Mg alloy subjected to sliding at elevated temperatures: a comparison between Al_2O_3 and MoS_2 nano additives in silicone oil-based lubricant," *Tribology International*, vol. 188, Article ID 108856, 2023.

[28] V. Y. Ulianitsky, D. V. Dudina, A. A. Shtertser, and I. Smurov, "Computer-controlled detonation spraying: flexible control of the coating chemistry and microstructure," *Metals*, vol. 9, no. 12, Article ID 1244, 2019.

[29] B. Rakhadilov, D. Buitkenov, Z. Sagdoldina, S. Kurbanbekov, and M. Adilkanova, "Structural features and tribological properties of detonation gun sprayed Ti–Si–C coating," *Coatings*, vol. 11, no. 2, Article ID 141, 2021.

[30] Y.-Z. Xing, Q.-L. Wei, and J.-M. Hao, "The fracture toughness of alumina coatings plasma-sprayed at different in situ temperatures," *Ceramics International*, vol. 38, no. 6, pp. 4661–4667, 2012.

[31] Y. Wang, C. Wu, L. Zhang, P. Qu, S. Li, and Z. Jiang, "Thermal oxidation and its effect on the wear of Mg alloy AZ31B," *Wear*, vol. 476, Article ID 203673, 2021.

[32] W. Li, L.-C. Zhang, C.-H. Wu, Z.-X. Cui, C. Niu, and Y. Wang, "Debris effect on the surface wear and damage evolution of counterpart materials subjected to contact sliding," *Advances in Manufacturing*, vol. 10, pp. 72–86, 2022.